Atmospheric
Chemistry
and Physics
Discussions

1 **Impact of cooking style and oil on semi-volatile and intermediate**

2 **volatility organic compound emissions from Chinese domestic cooking**

3 Kai Song[1,2], Song Guo[1,2,*], Yuanzheng Gong[1], Daqi Lv[1], Yuan Zhang[1], Zichao Wan[1], Tianyu Li[1],

4 Wenfei Zhu[1], Hui Wang[1], Ying Yu[1], Rui Tan[1], Ruizhe Shen[1], Sihua Lu[1], Shuangde Li[3], Yunfa Chen[3],

5 Min Hu[1,2]

6

7

8 [1] State Key Joint Laboratory of Environmental Simulation and Pollution Control, International Joint

9 Laboratory for Regional Pollution Control, Ministry of Education (IJRC), College of Environmental

10 Sciences and Engineering, *Beijing* 100871, China

11 [2] Collaborative Innovation Center of Atmospheric Environment and Equipment Technology, Nanjing

12 University of Information Science & Technology, *Nanjing* 210044, China

13 [3] State Key Laboratory of Multiphase Complex Systems, Institute of Process Engineering, Chinese

14 Academy of Sciences, *Beijing* 100190, China

15 * **Correspondence:** Song Guo: songguo@pku.edu.cn

16

17

Atmospheric
Chemistry
and Physics
Discussions

18 **Abstract:**

19   To elucidate the molecular chemical compositions, volatility-polarity distributions, as well as

20 influencing factors of Chinese cooking emissions, a comprehensive cooking emission experiment

21 was conducted. Semi-volatile and intermediate volatility organic compounds (S/IVOCs) from

22 cooking fumes were analyzed by a thermal desorption comprehensive two-dimensional gas

23 chromatography coupled with quadrupole mass spectrometer (TD-GC×GC-qMS). Emissions from

24 four typical Chinese dishes, i.e., fried chicken, Kung Pao chicken, pan-fried tofu, and stir-fried

25 cabbage were investigated to illustrate the impact of cooking style and material. Fumes of chicken

26 fried with corn, peanut, soybean, and sunflower oils were investigated to demonstrate the influence

27 of cooking oil. A total of 201 chemicals were quantified. Dishes cooked by stir-frying or deep-frying

28 cooking styles emit much more pollutants than relatively mild cooking methods. Aromatics and

29 oxygenated compounds were extensively detected among meat-related cooking fumes, while a

30 vegetable-related profile was observed in the emissions of stir-fried cabbage. The volatility-polarity

31 distributions of the four dish emissions were quite similar, yet the distributions diverged when

32 different types of oils were utilized. Ozone formation potential (OFP) was dominated by chemicals

33 in the VOC range. 10.2% - 32.0% of the SOA estimation could be explained by S/IVOCs.

34 Pixel-based partial least squares-discriminant analysis (PLS-DA) and multiway principal component

35 analysis (MPCA) were utilized for sample classification and key components identification. The

36 results indicated that the oil factor explained more variance of chemical compositions than the

37 cooking style factor. MPCA results emphasize the importance of the unsaturated fatty

38 acid-alkadienal-volatile products mechanism (oil autooxidation) accelerated by the cooking and

39 heating procedure.

40

41 **Keywords:** Cooking emissions; Semi-volatile organic compounds; Intermediate volatility organic

42 compounds; Cooking style; Oil

43

44

45

1 Introduction

46

47   Organics are key components of urban particles (Guo et al., 2014; Tang et al., 2018). Source

48 apportionment results indicated that vehicle exhaust is one of the important sources of gaseous and

49 particulate organics (Guo et al., 2020; Hu et al., 2015). However, the importance of cooking

50 emissions is rising due to the high impact on both primary precursor emissions and secondary

51 formation (Zhu et al., 2021). Cooking emitted organics are complex mixtures covering a wides range

52 of volatility, including volatile organic compounds (VOCs, organics with effective saturation

53 concentration higher than 10^6 μg m^{-3}) (Bruns et al., 2016; Fullana et al., 2004; Huang et al., 2011; Lu

54 et al., 2021; Zhang et al., 2019), intermediate volatility organic compounds (IVOCs, organics with

55 effective saturation concentration in the range of 10^3 -10^6 μg m^{-3}) (Liu et al., 2018; Lu et al., 2021;

56 Schauer et al., 2002), and semi-volatile organic compounds (SVOCs, organics with effective

57 saturation concentration in the range of 10^{-1} -10^3 μg m^{-3}) (Liu et al., 2018; Lu et al., 2021; Ma et al.,

58 2021; Schauer et al., 2002; Vicente et al., 2021). Along with a large variety of volatility, these

59 organics are also a large pool of complex components of different polarities, such as alkanes with

60 lower polarity (Gysel et al., 2018; Lin et al., 2010; Wang et al., 2015), polycyclic aromatics with

61 intermediate polarity (Chen et al., 2019; Kim et al., 2013; Wei See et al., 2006), acids, ketones, and

62 aldehydes with higher polarity (Alves et al., 2012; Gysel et al., 2018; He et al., 2004; Peng et al.,

63 2017). Such cooking-related organics are key pollutants exhibiting health effects (Gligorovski et al.,

64 2018; Huang et al., 2011; Zhao and Zhao, 2018) and air-quality problems (Abdullahi et al., 2013;

65 Zhao and Zhao, 2018). Although chemical compositions, fingerprints, and influencing factors of

66 cooking emissions have been clarified in some previous studies (Alves et al., 2021; Klein et al.,

67 2016a; Peng et al., 2017; Vicente et al., 2021), there are still questions that remain uncertain. The

68 first constrain is that resolving complex mixtures of cooking emissions is a tough job. Most

69 components in traditional gas chromatography-mass spectrometer (GC-MS) chromatograms remain

70 unresolved (Takhar et al., 2021; Zhao et al., 2014). It is of vital importance to identify chemical

71 compositions of unresolved complex mixtures (UCM) to better comprehend their contributions to

72 secondary organic aerosol (SOA). Particle-phase SVOC organics from cooking emissions are widely

73 demonstrated yet few studies focus on gas-phase IVOC or SVOC ones. Meanwhile, current studies

74 mainly focus on a single kind or a series of homologs (aldehydes (Abdullahi et al., 2013; Klein et al.,

75 2016a; Peng et al., 2017), alkanes (Abdullahi et al., 2013), or acids (Abdullahi et al., 2013; Takhar et

76 al., 2021; Zeng et al., 2020)). In other words, currently, there is no comprehensive source profile of

77 cooking emissions covering VOCs, IVOCs, and SVOCs.

78 The volatility-based method originated from the volatility-based set (VBS) is widely used to

79 demonstrate IVOC or SVOC emissions from different sources (Zhao et al., 2014, 2017), yet

80 chemical compositions from cooking emissions could not be demonstrated well only from the

81 volatility perspective. Large proportions of acids, esters, polycyclic aromatic hydrocarbons (PAHs),

82 and n-alkanes expand a wide range of polarity. A novel scheme combining volatility and polarity

83 should be developed to better figure out source emission characteristics.

84 Besides, it is well-known that cooking emissions vary dramatically with cooking style,

85 ingredients, food, oil, and temperature (Amouei Torkmahalleh et al., 2017; Klein et al., 2016b; Liu et

86 al., 2018; Takhar et al., 2021; Zhao et al., 2007b). Cooking style and oil are typical influencing

87 factors dominating the compositions of cooking fume (Klein et al., 2016a; Takhar et al., 2021; Zhang

88 et al., 2019). Some studies demonstrated the emission patterns of cooking fumes emphasizing the

89 influence of different dishes or cooking methods (Chen et al., 2018; Wang et al., 2020), and several

90 studies clarified the importance of n-alkanes (Zhao et al., 2007a), polycyclic aromatic hydrocarbons

91 (PAHs) (Abdel-Shafy and Mansour, 2016; Abdullahi et al., 2013), aldehydes (Katragadda et al., 2010;

92 Peng et al., 2017), and acids (Pei et al., 2016; Zeng et al., 2020; Zhao et al., 2007a) from cooking

93 emissions using various kinds of oils. However, few comprehensive investigations have been

94 reported that speciated the dominant influencing factor under multiple conditions of cooking

95 procedures.

96 In this work, a thermal desorption comprehensive two-dimensional gas chromatography

97 coupled with quadrupole mass spectrometer (TD-GC×GC-qMS) is utilized to resolve and quantify

98 gaseous organic emissions from the molecular level. GC×GC has been proved to be a powerful

99 technique to resolve UCM in previous studies (Cordero et al., 2018; Zhang et al., 2021a). A

100 two-dimensional panel combining the volatility and polarity properties of chemicals is developed to

101 better understand organic emissions. The ozone formation potential (OFP) and SOA formation from

102   gaseous precursors were estimated. To elucidate the main influencing factor of cooking emissions,

103   pixel-based partial least squares-discriminant analysis (PLS-DA) was utilized. The main chemical

104   reactions of cooking emission were further demonstrated by pixel-based multiway principal

105   component analysis (MPCA).

2   Experimental Desrciption

2.1   Sampling and quantification

108   Four typical Chinese dishes, i.e., fried chicken, Kung Pao chicken, pan-fried tofu, and stir-fried

109   cabbage, were cooked in corn oil in the laboratory of the Institute of Process Engineering, Chinese

110   Academy of Sciences. The detailed cooking procedures could be found in Table S1 and elsewhere

111   (Zhang et al., 2021b). Meanwhile, four types of oil (i.e., soybean, corn, sunflower, and peanut oil)

112   were used for frying chicken to comprehend the influence of oil. These four oils were chosen for

113   chicken-frying as they are commonly consumed in China (especially soybean oil) (Jamet and

114   Chaumet, 2016) and other countries worldwide (Awogbemi et al., 2019). Cooking fumes were mixed

115   with ambient air immediately in the kitchen ventilator and were sampled directly without dilution.

116   After collecting particles on quartz filters, gas-phase organics were sampled by pre-conditioned

117   Tenax TA tubes (Gerstel, Germany) with a flow of 0.5 L min^{-1}. A daily blank sampling of the air in

118   the kitchen ventilator was conducted before cooking and was subtracted in the quantification

119   procedure. All samples were frozen at -20℃ before analyzing.

120   A thermal desorption comprehensive two-dimensional gas chromatography coupled with

121   quadrupole mass spectrometer (TD-GC×GC-qMS, GC-MS TQ8050, Shimadzu, Japan) was utilized

122   for sample analysis with a desorption temperature of 280 ℃. The modulation period was 6s. See

123   more detail in Table S2. As the first and second columns of GC×GC were non-polar SH-Rxi-1ms (30

124   m × 0.25 mm × 0.25 μm) and polar BPX50 (2.5 m × 0.1 mm × 0.1 μm), the 1st retention time of a

125   chemical is related to its volatility while 2nd retention time is related to polarity (Nabi et al., 2014;

126   Nabi and Arey, 2017; Zushi et al., 2016). The total chromatogram was cut into volatility bins (B9 to

127   B31 with a decrease in volatility) following the pipeline of previous studies (Tang et al., 2021; Zhao

128   et al., 2014, 2017, 2018), while it was cut into slices by an increase of 0.5 s in the second retention

129   time (called 2D bins, from P1 to P12 with an increase of polarity). A two-dimensional panel was

130   developed in this way to investigate the emission of contaminants from aspects of their volatility and

131   polarity properties.

132   326 kinds of chemicals were qualified and quantified (Table S3) while 201 kinds of

133   contaminants were detected (Table S4) in cooking fumes covering a wide range of VOCs, IVOCs,

134   and SVOCs, including 25 aromatics, 19 *n*-alkanes, 100 oxygenated compounds (containing 7 acids,

135   10 alcohols, 29 aldehydes, 24 esters, 5 ketones, and others), 3 PAHs, and 54 other chemicals. The 1D

136   retention time shift of most chemicals is within 0.5 min, while the 2D retention time shift of most

137   chemicals is within 0.1s (Table S4), which is much less than the length of 1D (~ 8 min) and 2D (0.5s)

138   bins. Most of the R^2 of external calibration curves was between 0.90 – 1 (Table S5). Chemicals

139   without standards are semi-quantified by surrogates from the same class or *n*-alkanes in the same 1D

140   bins (Table S3). The uncertainties of semi-quantification of surrogates from the same class or

141   *n*-alkanes were 27% and 69% (Table S6). The average concentrations (μg m^{-3}) of (semi-)quantified

142   chemicals are listed in Table S4.

143   **2.2   Estimation of ozone and secondary organic aerosol (SOA) formation potential**

144   Ozone formation potential (OFP, μg m^{-3}) was calculated by the following equation (Atkinson

145   and Arey, 2003),

$$OFP = \sum [HC_i] \times MIR_i$$

146   Where $[HC_i]$ is the mass concentration of precursor i (μg m^{-3}) with maximum incremental

147   reactivity (MIR) of MIR_i. The MIR could be found in Table S3 and calculation procedures could be

148   found   inside   the   FOQAT   packages   developed   by   Tianshu   Chen

149   (https://github.com/tianshu129/foqat).

150   SOA (μg m^{-3}) was estimated by the following equation, where $[HC_i]$ is the mass concentration

151   of precursor i (μg m^{-3}) with OH reaction rate of $k_{OH,i}$, (cm^3 molecules^{-1} s^{-1}) and SOA yield of Y_i

152   (Table S3). The SOA yields of precursors were from literature (Algrim and Ziemann, 2016, 2019;

153   Chan et al., 2009, 2010; Harvey and Petrucci, 2015; Li et al., 2016; Liu et al., 2018; Loza et al., 2014;

154   Matsunaga et al., 2009; McDonald et al., 2018; Shah et al., 2020; Tkacik et al., 2012; Wu et al., 2017)

155   or surrogates from *n*-alkanes in the same volatility bins (Zhao et al., 2014, 2017). $[OH] \times \Delta t$ is the

156   OH exposure and was set to be 14.4 ×10^{10} molecules cm^{-3} s (~ 1.1 days in OH concentration of 1.5

157 $\times 10^6$ molecules cm^{-3}) in order to keep pace with our previous work (Zhang et al., 2021b; Zhu et al.,

158 2021).

$$SOA = \sum[HC_i] \times (1 - e^{-k_{OH,i} \times [OH] \times \Delta t}) \times Y_i \quad (2)$$

160 **2.3 Pixel-based analysis to demonstrate the main influencing factor of cooking emissions**

161 Pixel-based analysis was widely used as a dimension reduction tool for data interpretation

162 (Furbo et al., 2014). Pixel-based approaches have been proved to be powerful techniques for the

163 identification of atmospheric gaseous fingerprints (Song et al., 2022). In this work, pixel-based

164 partial least squares-discriminant analysis (PLS-DA) and multiway principal component analysis

165 (MPCA) were utilized for sample classification and key components identification, following the

166 pipeline of RGC×GC toolbox (Quiroz-Moreno et al., 2020). Chromatograms were imported in the

167 network common data form (netCDF) form by the interface of RGC×GC package. Smoothing,

168 baseline correction, alignment, and chromatogram unfolding were then conducted. MPCA was

169 calculated inside the R language, while PLS-DA was conducted by the interface of RGC×GC and

170 mixOmics packages (González et al., 2012; Lê Cao et al., 2009; Rohart et al., 2017). See more

171 information about the data processing procedure elsewhere (Quiroz-Moreno et al., 2020; Song et al.,

172 2022).

173 PLS-DA is a supervised method for the classification of grouped data. The main influencing

174 factor could be apportioned if one separation results of PLS-DA is much better than the other. MPCA

175 composes matrix $X_{(i,j)}$ into score (S) and loading (L) matrices. Pixel-based MPCA could identify the

176 similarities by resolving chemicals from the positive loading chromatogram (Song et al., 2022).

177 All data processing was accomplished by GC Image® (GC×GC Software, 2.8r2, USA) and R

178 4.1.0 (Chen, 2021; Patil, 2021; R Core Team, 2020).

179 **3 Results and discussions**

180 **3.1 Molecular compositions of S/IVOCs, OFP, and SOA estimation from different dish fumes**

181 Typical chromatograms of four dish emissions are displayed in Figure S1. Chemicals identified

182 are colored in groups in Figure 1. A typical system blank chromatogram is displayed in Figure S2.

183 The total mass concentrations of four dishes are displayed in Figure S3. Kung Pao chicken emitted

184 the most gaseous pollutants (461.2 ± 394.9 μg m^{-3}), followed by fried chicken (321.8 ± 220.6 μg m^{-3}),

Atmospheric
Chemistry
and Physics
Discussions

185   pan-fried tofu (257.0 ± 253.9 µg m^{-3}), and stir-fried cabbage (46.5 ± 36.5 µg m^{-3}). Stir-frying

186   procedures of Kung Pao chicken were rather intense, followed by deep-frying chicken. Research has

187   revealed that VOC emissions from quick- and stir-frying or deep-frying cooking methods are much

188   higher than those emitted from relatively mild cooking methods (Chen et al., 2018; Ciccone et al.,

189   2020; Lu et al., 2021).

190   The compositions of the gaseous emissions are exhibited in Figure S4. Aromatics contributed

191   59.1%, 23.7%, 8.1%, and 11.8% of the total mass concentration of Kung Pao chicken, fried chicken,

192   pan-fried tofu, and stir-fried cabbage, while oxygenated compounds accounted for 17.1%, 53.7%,

193   76.9%, and 25.0% of the total concentration, respectively. Compositions of organic emissions

194   diverged significantly and showed a great influence pattern of cooking styles (Wang et al., 2020).

195   Dishes cooked by intense cooking methods, like stir-frying, released more aromatics, while mild

196   cooking styles emitted more oxygenated compounds. Despite this, researches have indicated that the

197   emission patterns of different cooking styles are heavily driven by the thin or thick layer of oil (oil

198   amount), oil temperature, evaporation of water during cooking, and chemical reactions, such as

199   starch gelatinization, and protein denaturation (Atamaleki et al., 2021; Zhang et al., 2020). As for

200   chemical species, toluene, hexanoic acid, and pentanoic acid were extensively detected among

201   meat-related cooking fumes, which were among the top 5 species and accounted for more than half

202   of the total mass concentration. A vegetable-related pattern was observed in the emissions of

203   stir-fried cabbage. Alkanes (C10 – C12), alcohols (linalool, butanol), and pinenes (beta-pinene) were

204   the dominant chemical classes. As much as 26.3% and 26.1% of the total organics of stir-fried

205   cabbage emission were alkanes and alkenes (especially pinenes). The high plant wax content (Zhao

206   et al., 2007a) in this dish dramatically influenced the composition of the fume.

207   Although the profiles of compositions diverged from dish to dish, their volatility-polarity

208   patterns remained similar. The volatility-polarity distributions of the gaseous emissions are displayed

209   in Figure 2. VOCs (B11 and before) with low polarity (P1 – P4) dominated the emissions of

210   gas-phase contaminants. Chemicals in the VOC range accounted for 88.7%, 95.6%, 85.2%, and 81.4%

211   of the total mass concentration of fried chicken, Kung Pao chicken, pan-fried tofu, and stir-fried

212   cabbage emissions, while S/IVOCs accounted for 11.3%, 4.3%, 14.8%, and 18.6%, respectively.

213   The total mass concentration, compositions, and volatility-polarity distributions of OFP and

214   SOA estimation by gaseous precursors are displayed in Figure S3, Figure S4, and Figure 2,

215   respectively. The total OFP and SOA estimation are consistent with the mass concentration, as Kung

216   Pao chicken emitted the most pollutants and produced the most ozone formation (1408.3 ± 1296.5 µg

217   m^{-3}) and SOA formation (38.9 ± 32.1 µg m^{-3}). Pan-fried tofu emitted a little bit less than fried

218   chicken, yet produced more SOA estimation due to a large proportion of short-chain acids (hexanoic

219   acid). The short-chain acids are likely derived from scission reactions of allylic hydroperoxides

220   originated from unsaturated fatty acids (Chow, 2007; Goicoechea and Guillén, 2014). Although

221   chemicals in the VOC range dominated ozone and SOA formation, an enhancement of ozone

222   formation contribution and a decrease of SOA formation contribution were observed. VOCs

223   contributed more than 90% of the ozone estimation, and 68.0% - 89.8% of the total SOA estimation.

224   S/IVOCs explained 10.2% - 32.0% of the SOA estimation. Aromatics (toluene) and alkenes (heptene)

225   were dominant ozone formation precursors in meat-relating dishes (fried chicken, Kung Pao chicken,

226   and pan-fried tofu), while alcohols (butanol and linalool) were predominant for stir-fried cabbage.

227   Acids (hexanoic acid), aromatics (toluene), alkenes (pinenes), and alkanes were important SOA

228   precursors.

229   **3.2   Molecular compositions of S/IVOCs, OFP, and SOA estimation from fried chicken fumes**

230   **using four types of oils**

231   Typical chromatograms of fried chicken emissions cooked with corn, peanut, soybean and

232   sunflower oils are displayed in Figure S5. Chemicals identified are colored in groups in Figure S6.

233   Total chemical concentrations were 321.8 ± 220.6 µg m^{-3}, 228.2 ± 65.9 µg m^{-3}, 241.7 ± 122.3 µg m^{-3},

234   and 151.2 µg m^{-3} (n = 1) for chicken fried with corn, peanut, soybean, and sunflower oils,

235   respectively (Figure S7). Chicken fried with corn oil emitted the most abundant gaseous

236   contaminants. The emission patterns diverged from heated oil fumes as heated sunflower oil and

237   peanut oil emitted more organics (Liu et al., 2018). Compositions and volatility-polarity distributions

238   of contaminants are displayed in Figure S8 and Figure S9, respectively. Aromatic contributed 23.7%,

239   20.1%, 50.5%, and 19.8% of the total concentrations of fried chicken fumes cooked with corn,

240   peanut, soybean, and sunflower, oils, respectively. Fried chicken fumes cooked with soybean and

241 corn oil were abundant in toluene (rank 1st). Butanol was the most abundant chemical when peanut

242 and sunflower oils were used for frying. A previous study indicated that benzene, toluene, and

243 ethylbenzene were the three dominant aromatics in kitchens (Huang et al., 2011; Yi et al., 2019).

244 Monocyclic aromatics are formed from linoleic and linolenic acyl groups in the oil (Atamaleki et al.,

245 2021; Uriarte and Guillén, 2010). The decomposition of linoleic and linolenic acid forms alkadienals

246 and the latter ones form aromatics once lose H_2O (Atamaleki et al., 2021; Zhang et al., 2019).

247 According to previous studies, soybean oil contains more unsaturated fatty acids, especially linolenic

248 acid (Kostik et al., 2013; Ryan et al., 2008). The aromatic concentrations and compositions of the

249 fried chicken fumes diverged accordingly (Chow, 2007). Oxygenated compounds were extensively

250 detected, which accounted for 53.7%, 33.1%, 24.7%, and 35.0% of the total mass concentration

251 (Figure S8). Short-chain acids and aldehydes were the most abundant oxygenated compounds and

252 were dominated by hexanoic acid, hexanal, and nonanal. Despite acids and aldehydes, alcohols

253 (butanol, octenal) were heavily detected in the fume of corn oil-fried chicken, which was also

254 supported by another study (Liu et al., 2018; Reyes-Villegas et al., 2018). The short-chain

255 contaminants were fundamentally formed by hydroperoxide decomposition (originated from oleate

256 and linoleate in the oil) through homolytic scission or homolytic β-scission reactions (Chow, 2007;

257 Goicoechea and Guillén, 2014) and quickly evaporated from the oil. Either aromatics or oxygenated

258 compounds detected in the gas phase showed high sensitivity to oil compositions, especially

259 potentially influenced by oleic and linoleic compounds.

260   Although pollutants were dominated by aromatics, alkanes, and oxygenated compounds with

261 volatility bins of B9 to B12 (VOC-IVOC range) and polarity bins of P1 to P5 (low to medium

262 polarity), significant diversities of volatility-polarity distributions were observed (Figure S9). IVOCs

263 accounted for as much as 22.8% and 23.7% of the total mass concentration when peanut and

264 sunflower oils were utilized for frying. These two oils are more abundant in unsaturated fatty acids

265 (Kostik et al., 2013; Ryan et al., 2008). In contrast, the volatility-polarity distributions of dishes did

266 not vary much when corn oil was used for cooking. The volatility-polarity panels indicated that the

267 influence of oil might be much more effective than different cooking styles (dishes).

268   As for OFP estimation, chicken fried in soybean oil produced more ozone ($675.6 \pm 397.2 \ \mu g \ m^{-3}$)

269   due to the large proportion of aromatics. Chicken fried in corn oil emitted the most precursors and

270   produced the highest SOA formation (28.4 ± 18.0 μg m^{-3}). Aromatics were predominant in ozone

271   formation, while oxygenated compounds, alkenes, alkanes, and aromatics were important SOA

272   precursors. S/IVOCs were non-negligible SOA precursors because they contributed as much as

273   22.0%, 28.2%, 24.0%, and 29.7% of the SOA estimation. Without S/IVOCs, a large proportion of

274   SOA would be underestimated. Our work illustrated the importance of the measurement of S/IVOC

275   precursors which was absent in previous studies (Liu et al., 2018; Zhang et al., 2021b). Despite the

276   importance of aldehydes revealed in previous studies (Klein et al., 2016a; Liu et al., 2018), our

277   results demonstrated that alkanes, pinenes, and shott-chain acids are also key precursors in cooking

278   SOA reduction.

3.3   Elucidating the influencing factor and key reactions of cooking emissions

280   From the discussion above, cooking style and oil could influence emissions dramatically. But

281   we still wonder what is the main predominant factor shaping the profile of cooking emission. In

282   other words, we want to learn that does the cooking styles affect cooking patterns more, or vice versa?

283   A pixel-based partial least squares-discriminant analysis (PLS-DA) was utilized to investigate the

284   key factor. The results are displayed in Figure 3. PLS-DA is a supervised classification method

285   requiring the data pre-grouping. The separation results of the PLS-DA indicate the crucial pattern

286   behind the classification. When oil was set as the grouping variable, the separation was much better

287   than setting the dish as the grouping variable (Figure 3 (a) and (b)). The separation results

288   demonstrated that the oil used during the cooking procedure is much more crucial in shaping the

289   emission profiles than the cooking style. The varaince of cooking fumes could be largely explained

290   by the different oil utilized.

291   Plenty of physical and chemical reactions occur during the cooking procedure (Chow, 2007;

292   Goicoechea and Guillén, 2014). To demonstrate the direct effect of oil on cooking emission, PLS-DA

293   and MPCA analyses were utilized. The PLS-DA result showed that cooking emissions diverged from

294   oils (Figure 3 (c)), indicating that the physical reactions (evaporation) were not the main reactions

295   during the cooking procedure. MPCA results showed the chromatogram similarities (positive loading)

296   of oils and emissions. Fatty acids (palmitic acid, oleic acid, and linoleic acid), decanal, and

297 decadienals were the key fingerprints. The pattern is linked to the autooxidation procedure of oil. Oil

298 autooxidation is a three-step free radical process: initiation, propagation, and termination (Atamaleki

299 et al., 2021; Uriarte and Guillén, 2010; Yi et al., 2019). The key initiation step is the formation of

300 lipid radical (R•) from unsaturated fatty acid (RH). R• then react with O_2 to form peroxyl radical

301 (ROO•) and then form hydroperoxides (ROOH). Another RH changes to R• in this propagation

302 process. During the termination process, the decomposition of ROOH forms monomeric (keto-,

303 hydroxy-, and epoxy- derivatives), polymeric (RR, ROR, ROOR), and volatile compounds

304 (short-chain acids, aldehydes, alcohols, ketones). In more detail, the oxidation of unsaturated fatty

305 acids (such as linoleic acid) in oil leads to the production of alkadienals (such as (E,

306 E)-2,4-decadienal) which form aromatics (butylbenzene) by losing H_2O (Atamaleki et al., 2021;

307 Zhang et al., 2019). The short-chain aldehydes and acids are derived from scission reactions of

308 allylic hydroperoxides originated from unsaturated fatty acids (Chow, 2007; Goicoechea and Guillén,

309 2014), while the dehydration reaction of alkenals forms furanones (Zhang et al., 2019). Aldehydes,

310 acids, and furanones are regarded as potential tracers of cooking emissions (Klein et al., 2016a;

311 Wang et al., 2020; Zeng et al., 2020) and were widely detected in this work. These highly volatile

312 contaminants escape from oil immediately and lead to an accumulation of oxygenated compounds in

313 the gas-phase. Figure S10 showed the key reactions originating from linoleic acid. The key

314 chemicals elucidated by the MPCA analysis (Figure 3 (d)) demonstrated that the key chemical

315 reactions of cooking emissions are largely driven by the autooxidation of oil, which is accelerated

316 during the heating and cooking procedures (Atamaleki et al., 2021; Uriarte and Guillén, 2010; Yi et

317 al., 2019; Zhang et al., 2019).

318 **4   Atmospheric Implications**

319   To our best knowledge, this is the first time that gaseous VOCs, IVOCs, and SVOCs from

320 cooking fumes are quantified in detail. The influence of cooking style and oil is taken into

321 consideration in this work. S/IVOC species are key components as they contributed near a quarter of

322 the total SOA estimation. Previous works might underestimate the importance of cooking fumes to

323 SOA formation because only a series of IVOC homologs were quantified (Liu et al., 2018).

324   We also first proposed a novel two-dimensional panel elucidating the physiochemical properties

325   of contaminants from the perspectives of their volatilities and polarities. This novel scheme is

326   appropriate to demonstrate the complicated evolution of contaminants clearly and provide new

327   insight into the previously 1D-bins method. The volatility-polarity panel inherited the spirit of the

328   two-dimensional volatility-based set (2D-VBS) (Donahue et al., 2011, 2012) and would be further

329   implemented in the analysis of complex ambient or source samples along with the powerful

330   separating capacity of GC×GC. We also provide powerful tools in speciating the main driving factor

331   and key chemical reactions in rather complicated systems. The pixel-based PLS-DA and MPCA

332   analysis greatly enhance our learning of complex chromatograms and provide us with new insight

333   into the dimension reduction processes. The analyzing scheme could benefit those analysts with less

334   experience in GC×GC data processing.

335   Our results demonstrated that both cooking styles (dish) and oils influence the cooking

336   emissions. Dishes cooked by quick- and stir-frying or deep-frying cooking methods emit much more

337   gas-phase contaminants than relatively mild cooking methods. Cooking materials could also

338   influence the compositions of fumes as well. Aromatics and oxygenated compounds were

339   extensively detected among meat-related cooking fumes, while a vegetable-related pattern was

340   observed in the emissions of stir-fried cabbage. As much as 26.3% and 26.1% of the total organics of

341   stir-fried cabbage emission were alkanes and alkenes (especially pinenes). On the other hand, oils

342   greatly influence the composition and volatility-polarity distribution of pollutants. Chicken fried by

343   corn oil emitted the most abundant contaminants. However, the ozone formation from soybean-oil

344   fried chicken fumes was much higher. Considering the high consumption proportion of soybean oil

345   (~ 44% in volume of oil usage) in China (Jamet and Chaumet, 2016), the influence of using soybean

346   cooking oil on ozone formation might be underestimated. The PLS-DA and MPCA analysis indicated

347   the importance of edible oils on cooking emissions. If cooking-related pollution control strategies are

348   made, the suggestion of deduction of oils that contain more unsaturated fatty acids (such as soybean

349   oil) could be taken into consideration. The MPCA results also indicate that the heating and cooking

350   procedure greatly enhance the autooxidation of oil. MPCA results emphasize the importance of the

351   unsaturated fatty acid-alkadienal-volatile product mechanism.

352

Atmospheric
Chemistry
and Physics
Discussions

359 **Credit Author Statement:**

360 Kai Song, Yuanzheng Gong, and Daqi Lv conducted the experiments.

361 Kai Song and Yuanzheng Gong analyzed the data.

362 Kai Song, Song Guo, Yuanzheng Gong, Daqi Lv, Yuan Zhang, Zichao Wan, Tianyu Li, Wenfei Zhu,

363 Hui Wang, Ying Yu, Rui Tan, Ruizhe Shen, Sihua Lu, Shuangde Li, Yunfa Chen, and Min Hu

364 discussed the scientific results and review the paper.

365 Kai Song and Song Guo wrote the paper.

366

367 **Reference**

368 Abdel-Shafy, H. I. and Mansour, M. S. M.: A review on polycyclic aromatic hydrocarbons: Source,

369   environmental impact, effect on human health and remediation, Egypt. J. Pet., 25(1), 107–123,

370   doi:10.1016/J.EJPE.2015.03.011, 2016.

371 Abdullahi, K. L., Delgado-Saborit, J. M. and Harrison, R. M.: Emissions and indoor concentrations

372   of particulate matter and its specific chemical components from cooking: A review., 2013.

373 Algrim, L. B. and Ziemann, P. J.: Effect of the Keto Group on Yields and Composition of Organic

374   Aerosol Formed from OH Radical-Initiated Reactions of Ketones in the Presence of NOx, J.

375   Phys. Chem. A, 120(35), 6978–6989, doi:10.1021/acs.jpca.6b05839, 2016.

376 Algrim, L. B. and Ziemann, P. J.: Effect of the Hydroxyl Group on Yields and Composition of

377   Organic Aerosol Formed from OH Radical-Initiated Reactions of Alcohols in the Presence of

378   NOx, ACS Earth Sp. Chem., 3(3), 413–423, doi:10.1021/acsearthspacechem.9b00015, 2019.

379 Alves, C., Vicente, A., Pio, C., Kiss, G., Hoffer, A., Decesari, S., Prevôt, A. S. H., Minguillón, M. C.,

380   Querol, X., Hillamo, R., Spindler, G. and Swietlicki, E.: Organic compounds in aerosols from

Atmospheric
Chemistry
and Physics
Discussions

381   selected European sites - Biogenic versus anthropogenic sources, Atmos. Environ., 59, 243–255,

382   doi:10.1016/J.ATMOSENV.2012.06.013, 2012.

383 Alves, C. A., Vicente, E. D., Evtyugina, M., Vicente, A. M. P., Sainnokhoi, T. A. and Kováts, N.:

384   Cooking activities in a domestic kitchen: Chemical and toxicological profiling of emissions, Sci.

385   Total Environ., 772, 145412, doi:10.1016/j.scitotenv.2021.145412, 2021.

386 Amouei Torkmahalleh, M., Gorjinezhad, S., Unluevcek, H. S. and Hopke, P. K.: Review of factors

387   impacting emission/concentration of cooking generated particulate matter, , 586, 1046–1056,

388   doi:10.1016/J.SCITOTENV.2017.02.088, 2017.

389 Atamaleki, A., Motesaddi Zarandi, S., Massoudinejad, M., Samimi, K., Fakhri, Y., Ghorbanian, M.

390   and Mousavi Khaneghah, A.: The effect of frying process on the emission of the volatile organic

391   compounds and monocyclic aromatic group (BTEX), Int. J. Environ. Anal. Chem., 1–14,

392   doi:10.1080/03067319.2021.1950148, 2021.

393 Atkinson, R. and Arey, J.: Atmospheric Degradation of Volatile Organic Compounds, Chem. Rev.,

394   103(12), 4605–4638, doi:10.1021/cr0206420, 2003.

395 Awogbemi, O., Onuh, E. I. and Inambao, F. L.: Comparative study of properties and fatty acid

396   composition of some neat vegetable oils and waste cooking oils, Int. J. Low-Carbon Technol.,

397   14(3), 417–425, doi:10.1093/ijlct/ctz038, 2019.

398 Bruns, E. A., El Haddad, I., Slowik, J. G., Kilic, D., Klein, F., Baltensperger, U. and Prévôt, A. S. H.:

399   Identification of significant precursor gases of secondary organic aerosols from residential wood

400   combustion, Sci. Rep., 6, doi:10.1038/srep27881, 2016.

401 Chan, A. W. H., Kautzman, K. E., Chhabra, P. S., Surratt, J. D., Chan, M. N., Crounse, J. D., Kürten,

402   A., Wennberg, P. O., Flagan, R. C. and Seinfeld, J. H.: Secondary organic aerosol formation

403   from photooxidation of naphthalene and alkylnaphthalenes: Implications for oxidation of

404   intermediate volatility organic compounds (IVOCs), Atmos. Chem. Phys., 9(9), 3049–3060,

405   doi:10.5194/acp-9-3049-2009, 2009.

406 Chan, A. W. H., Chan, M. N., Surratt, J. D., Chhabra, P. S., Loza, C. L., Crounse, J. D., Yee, L. D.,

407   Flagan, R. C., Wennberg, P. O. and Seinfeld, J. H.: Role of aldehyde chemistry and NOx

408   concentrations in secondary organic aerosol formation, Atmos. Chem. Phys., 10(15), 7169–7188,

409   doi:10.5194/ACP-10-7169-2010, 2010.

410   Chen, C., Zhao, Y. and Zhao, B.: Emission Rates of Multiple Air Pollutants Generated from Chinese

411   Residential Cooking, Environ. Sci. Technol., 52(3), 1081–1087, doi:10.1021/acs.est.7b05600,

412   2018.

413   Chen, C. Y., Kuo, Y. C., Wang, S. M., Wu, K. R., Chen, Y. C. and Tsai, P. J.: Techniques for

414   predicting exposures to polycyclic aromatic hydrocarbons (PAHs) emitted from cooking

415   processes for cooking workers, Aerosol Air Qual. Res., 19(2), 307–317,

416   doi:10.4209/aaqr.2018.09.0346, 2019.

417   Chen, T.: foqat: Field Observation Quick Analysis Toolkit, [online] Available from:

418   https://doi.org/10.5281/zenodo.4735828, 2021.

419   Chow, C. K.: Fatty acids in foods and their health implications, third edition., 2007.

420   Ciccone, M., Chambers, D., Chambers, E. and Talavera, M.: Determining which cooking method

421   provides the best sensory differentiation of potatoes, Foods, 9(4), doi:10.3390/foods9040451,

422   2020.

423   Cordero, C., Schmarr, H. G., Reichenbach, S. E. and Bicchi, C.: Current Developments in Analyzing

424   Food Volatiles by Multidimensional Gas Chromatographic Techniques, J. Agric. Food Chem.,

425   66(10), 2226–2236, doi:10.1021/acs.jafc.6b04997, 2018.

426   Donahue, N. M., Epstein, S. A., Pandis, S. N. and Robinson, A. L.: A two-dimensional volatility

427   basis set: 1. organic-aerosol mixing thermodynamics, Atmos. Chem. Phys., 11(7), 3303–3318,

428   doi:10.5194/acp-11-3303-2011, 2011.

429   Donahue, N. M., Kroll, J. H., Pandis, S. N. and Robinson, A. L.: A two-dimensional volatility basis

430   set-Part 2: Diagnostics of organic-aerosol evolution, Atmos. Chem. Phys., 12(2), 615–634,

431   doi:10.5194/acp-12-615-2012, 2012.

432   Fullana, A., Carbonell-Barrachina, A. A. and Sidhu, S.: Comparison of volatile aldehydes present in

433   the cooking fumes of extra virgin olive, olive, and canola oils, J. Agric. Food Chem., 52(16),

434   5207–5214, doi:10.1021/JF035241F, 2004.

435   Furbo, S., Hansen, A. B., Skov, T. and Christensen, J. H.: Pixel-based analysis of comprehensive

436   two-dimensional gas chromatograms (color plots) of petroleum: A tutorial, Anal. Chem., 86(15),

437   7160–7170, doi:10.1021/ac403650d, 2014.

438   Gligorovski, S., Li, X. and Herrmann, H.: Indoor (Photo)chemistry in China and Resulting Health

439   Effects, Environ. Sci. Technol., 52(19), 10909–10910, doi:10.1021/acs.est.8b04739, 2018.

440   Goicoechea, E. and Guillén, M. D.: Volatile compounds generated in corn oil stored at room

441   temperature. Presence of toxic compounds, Eur. J. Lipid Sci. Technol., 116(4), 395–406,

442   doi:10.1002/ejlt.201300244, 2014.

443   González, I., Cao, K. A. L., Davis, M. J. and Déjean, S.: Visualising associations between paired

444   "omics" data sets, BioData Min., 5(1), doi:10.1186/1756-0381-5-19, 2012.

445   Guo, S., Hu, M., Zamora, M. L., Peng, J., Shang, D., Zheng, J., Du, Z., Wu, Z., Shao, M., Zeng, L.,

446   Molina, M. J. and Zhang, R.: Elucidating severe urban haze formation in China, Proc. Natl.

447   Acad. Sci. U. S. A., 111(49), 17373–17378, doi:10.1073/pnas.1419604111, 2014.

448   Guo, S., Hu, M., Peng, J., Wu, Z., Zamora, M. L., Shang, D., Du, Z., Zheng, J., Fang, X., Tang, R.,

449   Wu, Y., Zeng, L., Shuai, S., Zhang, W., Wang, Y., Ji, Y., Li, Y., Zhang, A. L., Wang, W., Zhang,

450   F., Zhao, J., Gong, X., Wang, C., Molina, M. J. and Zhang, R.: Remarkable nucleation and

451   growth of ultrafine particles from vehicular exhaust, Proc. Natl. Acad. Sci. U. S. A., 117(7),

452   3427–3432, doi:10.1073/pnas.1916366117, 2020.

453   Gysel, N., Dixit, P., Schmitz, D. A., Engling, G., Cho, A. K., Cocker, D. R. and Karavalakis, G.:

454   Chemical speciation, including polycyclic aromatic hydrocarbons (PAHs), and toxicity of

455   particles emitted from meat cooking operations, Sci. Total Environ., 633, 1429–1436,

456   doi:10.1016/j.scitotenv.2018.03.318, 2018.

457   Harvey, R. M. and Petrucci, G. A.: Control of ozonolysis kinetics and aerosol yield by nuances in the

458   molecular structure of volatile organic compounds, Atmos. Environ., 122, 188–195,

459   doi:10.1016/j.atmosenv.2015.09.038, 2015.

460   He, L. Y., Hu, M., Wang, L., Huang, X. F. and Zhang, Y. H.: Characterization of fine organic

461   particulate matter from Chinese cooking, J. Environ. Sci., 16(4), 570–575, 2004.

462   Hu, M., Guo, S., Peng, J. F. and Wu, Z. J.: Insight into characteristics and sources of PM2.5 in the

463   Beijing-Tianjin-Hebei region, China, Natl. Sci. Rev., 2(3), 257–258, doi:10.1093/nsr/nwv003,

464   2015.

465   Huang, Y., Ho, S. S. H., Ho, K. F., Lee, S. C., Yu, J. Z. and Louie, P. K. K.: Characteristics and

466   health impacts of VOCs and carbonyls associated with residential cooking activities in Hong

467   Kong, J. Hazard. Mater., 186(1), 344–351, doi:10.1016/j.jhazmat.2010.11.003, 2011.

468   Jamet, J. P. and Chaumet, J. M.: Soybean in China: Adaptating to the liberalization, OCL - Oilseeds

469   fats, Crop. Lipids, 23(6), doi:10.1051/ocl/2016044, 2016.

470   Katragadda, H. R., Fullana, A., Sidhu, S. and Carbonell-Barrachina, Á. A.: Emissions of volatile

471   aldehydes from heated cooking oils, Food Chem., 120(1), 59–65,

472   doi:10.1016/j.foodchem.2009.09.070, 2010.

473   Kim, K. H., Jahan, S. A., Kabir, E. and Brown, R. J. C.: A review of airborne polycyclic aromatic

474   hydrocarbons (PAHs) and their human health effects, Elsevier Ltd., 2013.

475   Klein, F., Platt, S. M., Farren, N. J., Detournay, A., Bruns, E. A., Bozzetti, C., Daellenbach, K. R.,

476   Kilic, D., Kumar, N. K., Pieber, S. M., Slowik, J. G., Temime-Roussel, B., Marchand, N.,

477   Hamilton, J. F., Baltensperger, U., Prévôt, A. S. H. H., El Haddad, I., Haddad, I. El and El

478   Haddad, I.: Characterization of Gas-Phase Organics Using Proton Transfer Reaction

479   Time-of-Flight Mass Spectrometry: Cooking Emissions, Environ. Sci. Technol., 50(3), 1243–

480   1250, doi:10.1021/acs.est.5b04618, 2016a.

481   Klein, F., Farren, N. J., Bozzetti, C., Daellenbach, K. R., Kilic, D., Kumar, N. K., Pieber, S. M.,

482   Slowik, J. G., Tuthill, R. N., Hamilton, J. F., Baltensperger, U., Prévôt, A. S. H. and El Haddad,

483   I.: Indoor terpene emissions from cooking with herbs and pepper and their secondary organic

484   aerosol production potential, Sci. Rep., 6, doi:10.1038/srep36623, 2016b.

485   Kostik, V., Memeti, S. and Bauer, B.: Fatty acid composition of edible oils and fats, J. Hyg. Eng.

486   Des., 4, 112–116, 2013.

487   Lê Cao, K. A., González, I. and Déjean, S.: IntegrOmics: An R package to unravel relationships

488   between two omics datasets, Bioinformatics, 25(21), 2855–2856,

489   doi:10.1093/bioinformatics/btp515, 2009.

490   Li, L., Tang, P., Nakao, S. and Cocker, D. R.: Impact of molecular structure on secondary organic

491   aerosol formation from aromatic hydrocarbon photooxidation under low-NOx conditions, Atmos.

492   Chem. Phys., 16(17), 10793–10808, doi:10.5194/acp-16-10793-2016, 2016.

493   Lin, Y., Shao, M. and Lu, S.: The emission characteristics of hydrocarbon from Chinese cooking

494   under smoke control, Int. J. Environ. Anal. Chem., 90(9), 708–721,

495   doi:10.1080/03067310903194964, 2010.

496   Liu, T., Wang, Z., Huang, D. D., Wang, X. and Chan, C. K.: Significant Production of Secondary

497   Organic Aerosol from Emissions of Heated Cooking Oils, Environ. Sci. Technol. Lett., 5(1), 32–

498   37, doi:10.1021/acs.estlett.7b00530, 2018.

499   Loza, C. L., Craven, J. S., Yee, L. D., Coggon, M. M., Schwantes, R. H., Shiraiwa, M., Zhang, X.,

500   Schilling, K. A., Ng, N. L., Canagaratna, M. R., Ziemann, P. J., Flagan, R. C. and Seinfeld, J. H.:

501   Secondary organic aerosol yields of 12-carbon alkanes, Atmos. Chem. Phys., 14(3), 1423–1439,

502   doi:10.5194/acp-14-1423-2014, 2014.

503   Lu, F., Shen, B., Li, S., Liu, L., Zhao, P. and Si, M.: Exposure characteristics and risk assessment of

504   VOCs from Chinese residential cooking, J. Environ. Manage., 289, 112535,

505   doi:10.1016/J.JENVMAN.2021.112535, 2021.

506   Ma, S., Yue, C., Tang, J., Lin, M., Zhuo, M., Yang, Y., Li, G. and An, T.: Occurrence and

507   distribution of typical semi-volatile organic chemicals (SVOCs) in paired indoor and outdoor

508   atmospheric fine particle samples from cities in southern China, Environ. Pollut., 269,

509   doi:10.1016/J.ENVPOL.2020.116123, 2021.

510   Matsunaga, A., Docherty, K. S., Lim, Y. B. and Ziemann, P. J.: Composition and yields of secondary

511   organic aerosol formed from OH radical-initiated reactions of linear alkenes in the presence of

512   NOx: Modeling and measurements, Atmos. Environ., 43(6), 1349–1357,

513   doi:10.1016/j.atmosenv.2008.12.004, 2009.

514   McDonald, B. C., De Gouw, J. A., Gilman, J. B., Jathar, S. H., Akherati, A., Cappa, C. D., Jimenez,

515   J. L., Lee-Taylor, J., Hayes, P. L., McKeen, S. A., Cui, Y. Y., Kim, S. W., Gentner, D. R.,

516   Isaacman-VanWertz, G., Goldstein, A. H., Harley, R. A., Frost, G. J., Roberts, J. M., Ryerson, T.

517   B. and Trainer, M.: Volatile chemical products emerging as largest petrochemical source of

518   urban organic emissions, Science (80-.)., 359(6377), 760–764, doi:10.1126/science.aaq0524,

519   2018.

520   Nabi, D. and Arey, J. S.: Predicting Partitioning and Diffusion Properties of Nonpolar Chemicals in

Atmospheric
Chemistry
and Physics
Discussions

521   Biotic Media and Passive Sampler Phases by GC ×GC, Environ. Sci. Technol., 51(5), 3001–

522   3011, doi:10.1021/acs.est.6b05071, 2017.

523   Nabi, D., Gros, J., Dimitriou-Christidis, P. and Arey, J. S.: Mapping environmental partitioning

524   properties of nonpolar complex mixtures by use of GC ×GC, Environ. Sci. Technol., 48(12),

525   6814–6826, doi:10.1021/es501674p, 2014.

526   Patil, I.: Visualizations with statistical details: The "ggstatsplot" approach, J. Open Source Softw.,

527   6(61), 3167, doi:10.21105/joss.03167, 2021.

528   Pei, B., Cui, H., Liu, H. and Yan, N.: Chemical characteristics of fine particulate matter emitted from

529   commercial cooking, Front. Environ. Sci. Eng., 10(3), 559–568,

530   doi:10.1007/s11783-016-0829-y, 2016.

531   Peng, C. Y., Lan, C. H., Lin, P. C. and Kuo, Y. C.: Effects of cooking method, cooking oil, and food

532   type on aldehyde emissions in cooking oil fumes, J. Hazard. Mater., 324, 160–167,

533   doi:10.1016/J.JHAZMAT.2016.10.045, 2017.

534   Quiroz-Moreno, C., Furlan, M. F., Belinato, J. R., Augusto, F., Alexandrino, G. L. and Mogollón, N.

535   G. S.: RGCxGC toolbox: An R-package for data processing in comprehensive two-dimensional

536   gas chromatography-mass spectrometry, Microchem. J., 156, 104830,

537   doi:10.1016/j.microc.2020.104830, 2020.

538   R Core Team: R Core Team 2020 R: A language and environment for statistical computing. R

539   foundation for statistical computing. https://www.R-project.org/, , 2020 [online] Available from:

540   http://www.r-project.org/, 2020.

541   Reyes-Villegas, E., Bannan, T., Breton, M. Le, Mehra, A., Priestley, M., Percival, C., Coe, H., Allan,

542   J. D., Le Breton, M., Mehra, A., Priestley, M., Percival, C., Coe, H. and Allan, J. D.: Online

543   Chemical Characterization of Food-Cooking Organic Aerosols: Implications for Source

544   Apportionment, , 52(9), 5308–5318 [online] Available from:

545   https://pubs.acs.org/doi/full/10.1021/acs.est.7b06278 (Accessed 19 July 2021), 2018.

546   Rohart, F., Gautier, B., Singh, A. and Lê Cao, K. A.: mixOmics: an R package for 'omics feature

547   selection and multiple data integration, bioRxiv, 13(11), doi:10.1101/108597, 2017.

548   Ryan, L. C., Mestrallet, M. G., Nepote, V., Conci, S. and Grosso, N. R.: Composition, stability and

549   acceptability of different vegetable oils used for frying peanuts, Int. J. Food Sci. Technol., 43(2),

550   193–199, doi:10.1111/j.1365-2621.2006.01288.x, 2008.

551   Schauer, J. J., Kleeman, M. J., Cass, G. R. and Simoneit, B. R. T.: Measurement of emissions from

552   air pollution sources. 4. C1-C27 organic compounds from cooking with seed oils, Environ. Sci.

553   Technol., 36(4), 567–575, doi:10.1021/es002053m, 2002.

554   Shah, R. U., Coggon, M. M., Gkatzelis, G. I., McDonald, B. C., Tasoglou, A., Huber, H., Gilman, J.,

555   Warneke, C., Robinson, A. L. and Presto, A. A.: Urban Oxidation Flow Reactor Measurements

556   Reveal Significant Secondary Organic Aerosol Contributions from Volatile Emissions of

557   Emerging Importance, Environ. Sci. Technol., 54(2), 714–725, doi:10.1021/acs.est.9b06531,

558   2020.

559   Song, K., Gong, Y., Guo, S., Lv, D., Wang, H., Wan, Z., Yu, Y., Tang, R., Li, T., Tan, R., Zhu, W.,

560   Shen, R. and Lu, S.: Investigation of partition coefficients and fingerprints of atmospheric gas-

561   and particle-phase intermediate volatility and semi-volatile organic compounds using

562   pixel-based approaches, J. Chromatogr. A, 1665, 462808, doi:10.1016/j.chroma.2022.462808,

563   2022.

564   Takhar, M., Li, Y. and W. H. Chan, A.: Characterization of secondary organic aerosol from

565   heated-cooking-oil emissions: Evolution in composition and volatility, Atmos. Chem. Phys.,

566   21(6), 5137–5149, doi:10.5194/ACP-21-5137-2021, 2021.

567   Tang, R., Wu, Z. Z. Z. Z., Li, X., Wang, Y., Shang, D., Xiao, Y., Li, M., Zeng, L., Wu, Z. Z. Z. Z.,

568   Hallquist, M., Hu, M. and Guo, S.: Primary and secondary organic aerosols in summer 2016 in

569   Beijing, Atmos. Chem. Phys., 18(6), 4055–4068, doi:10.5194/acp-18-4055-2018, 2018.

570   Tang, R., Lu, Q., Guo, S., Wang, H., Song, K., Yu, Y., Tan, R., Liu, K., Shen, R., Chen, S., Zeng, L.,

571   Jorga, S. D., Zhang, Z., Zhang, W., Shuai, S. and Robinson, A. L.: Measurement report: Distinct

572   emissions and volatility distribution of intermediate-volatility organic compounds from on-road

573   Chinese gasoline vehicles: Implication of high secondary organic aerosol formation potential,

574   Atmos. Chem. Phys., 21(4), 2569–2583, doi:10.5194/acp-21-2569-2021, 2021.

575   Tkacik, D. S., Presto, A. A., Donahue, N. M. and Robinson, A. L.: Secondary organic aerosol

576   formation from intermediate-volatility organic compounds: Cyclic, linear, and branched alkanes,

577   Environ. Sci. Technol., 46(16), 8773–8781, doi:10.1021/es301112c, 2012.

578   Uriarte, P. S. and Guillén, M. D.: Formation of toxic alkylbenzenes in edible oils submitted to frying

579   temperature. Influence of oil composition in main components and heating time, Food Res. Int.,

580   43(8), 2161–2170, doi:10.1016/j.foodres.2010.07.022, 2010.

581   Vicente, A. M. P., Rocha, S., Duarte, M., Moreira, R., Nunes, T. and Alves, C. A.: Fingerprinting

582   and emission rates of particulate organic compounds from typical restaurants in Portugal, Sci.

583   Total Environ., 778, 146090, doi:10.1016/J.SCITOTENV.2021.146090, 2021.

584   Wang, G., Cheng, S., Wei, W., Wen, W., Wang, X. and Yao, S.: Chemical characteristics of fine

585   particles emitted from different chinese cooking styles, Aerosol Air Qual. Res., 15(6), 2357–

586   2366, doi:10.4209/aaqr.2015.02.0079, 2015.

587   Wang, L., Zhang, L., Ristovski, Z., Zheng, X., Wang, H., Li, L., Gao, J., Salimi, F., Gao, Y., Jing, S.,

588   Wang, L., Chen, J. and Stevanovic, S.: Assessing the Effect of Reactive Oxygen Species and

589   Volatile Organic Compound Profiles Coming from Certain Types of Chinese Cooking on the

590   Toxicity of Human Bronchial Epithelial Cells, Environ. Sci. Technol., 54(14), 8868–8877,

591   doi:10.1021/acs.est.9b07553, 2020.

592   Wei See, S., Karthikeyan, S. and Balasubramanian, R.: Health risk assessment of occupational

593   exposure to particulate-phase polycyclic aromatic hydrocarbons associated with Chinese, Malay

594   and Indian cooking, J. Environ. Monit., 8(3), 369–376, doi:10.1039/b516173h, 2006.

595   Wu, W., Zhao, B., Wang, S. and Hao, J.: Ozone and secondary organic aerosol formation potential

596   from anthropogenic volatile organic compounds emissions in China, J. Environ. Sci. (China), 53,

597   224–237, doi:10.1016/j.jes.2016.03.025, 2017.

598   Yi, H., Huang, Y., Tang, X., Zhao, S., Xie, X. and Zhang, Y.: Characteristics of non-methane

599   hydrocarbons and benzene series emission from commonly cooking oil fumes, Atmos. Environ.,

600   200, 208–220, doi:10.1016/j.atmosenv.2018.12.018, 2019.

601   Zeng, J., Yu, Z., Mekic, M., Liu, J., Li, S., Loisel, G., Gao, W., Gandolfo, A., Zhou, Z., Wang, X.,

602   Herrmann, H., Gligorovski, S. and Li, X.: Evolution of Indoor Cooking Emissions Captured by

603   Using Secondary Electrospray Ionization High-Resolution Mass Spectrometry, Environ. Sci.

604   Technol. Lett., 7(2), 76–81 [online] Available from:

Atmospheric
Chemistry
and Physics
Discussions

605   https://pubs.acs.org/doi/full/10.1021/acs.estlett.0c00044 (Accessed 19 July 2021), 2020.

606   Zhang, D. C., Liu, J. J., Jia, L. Z., Wang, P. and Han, X.: Speciation of VOCs in the cooking fumes

607   from five edible oils and their corresponding health risk assessments, Elsevier Ltd., 2019.

608   Zhang, X., Zhang, M. and Adhikari, B.: Recent developments in frying technologies applied to fresh

609   foods, Trends Food Sci. Technol., 98, 68–81, doi:10.1016/j.tifs.2020.02.007, 2020.

610   Zhang, X. Y., Lu, Y., Du, Y., Wang, W. L., Yang, L. L. and Wu, Q. Y.: Comprehensive

611   GC×GC-qMS with a mass-to-charge ratio difference extraction method to identify new

612   brominated byproducts during ozonation and their toxicity assessment, J. Hazard. Mater., 403,

613   doi:10.1016/j.jhazmat.2020.124103, 2021a.

614   Zhang, Z., Zhu, W., Hu, M., Wang, H., Chen, Z., Shen, R., Yu, Y., Tan, R. and Guo, S.: Secondary

615   Organic Aerosol from Typical Chinese Domestic Cooking Emissions, Environ. Sci. Technol.

616   Lett., 8(1), 24–31, doi:10.1021/acs.estlett.0c00754, 2021b.

617   Zhao, Y. and Zhao, B.: Emissions of air pollutants from Chinese cooking: A literature review,

618   Tsinghua University Press., 2018.

619   Zhao, Y., Hu, M., Slanina, S. and Zhang, Y.: Chemical compositions of fine particulate organic

620   matter emitted from Chinese cooking., 2007a.

621   Zhao, Y., Hu, M., Slanina, S. and Zhang, Y.: The molecular distribution of fine particulate organic

622   matter emitted from Western-style fast food cooking, Atmos. Environ., 41(37), 8163–8171,

623   doi:10.1016/j.atmosenv.2007.06.029, 2007b.

624   Zhao, Y., Hennigan, C. J., May, A. A., Tkacik, D. S., De Gouw, J. A., Gilman, J. B., Kuster, W. C.,

625   Borbon, A. and Robinson, A. L.: Intermediate-volatility organic compounds: A large source of

626   secondary organic aerosol, Environ. Sci. Technol., 48(23), 13743–13750,

627   doi:10.1021/es5035188, 2014.

628   Zhao, Y., Saleh, R., Saliba, G., Presto, A. A., Gordon, T. D., Drozd, G. T., Goldstein, A. H.,

629   Donahue, N. M. and Robinson, A. L.: Reducing secondary organic aerosol formation from

630   gasoline vehicle exhaust, Proc. Natl. Acad. Sci. U. S. A., 114(27), 6984–6989,

631   doi:10.1073/pnas.1620911114, 2017.

632   Zhao, Y., Lambe, A. T., Saleh, R., Saliba, G. and Robinson, A. L.: Secondary Organic Aerosol

Atmospheric
Chemistry
and Physics
Discussions

633   Production from Gasoline Vehicle Exhaust: Effects of Engine Technology, Cold Start, and

634   Emission Certification Standard, Environ. Sci. Technol., 52(3), 1253–1261,
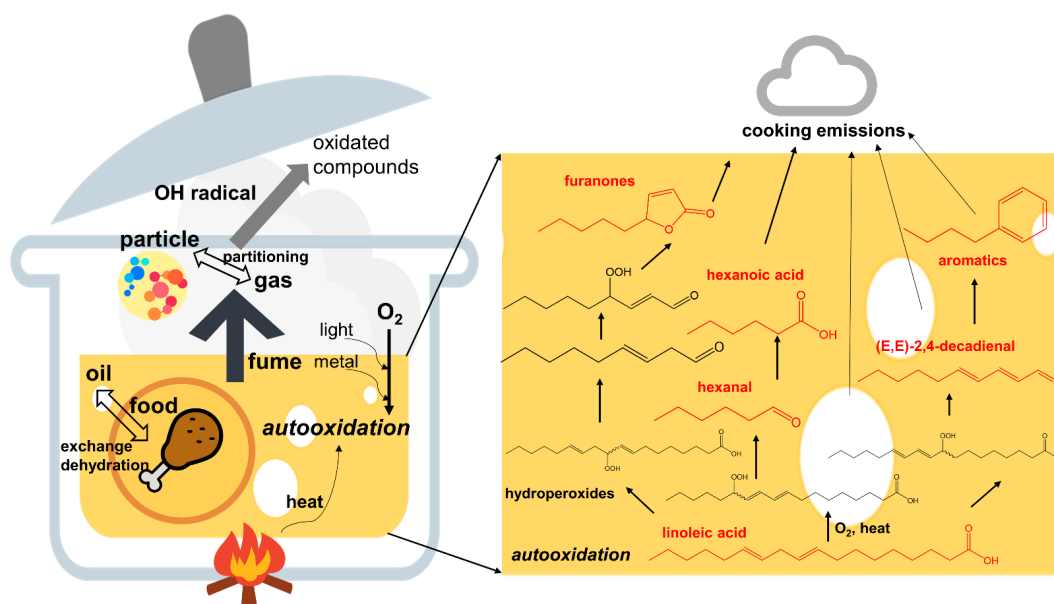
635   doi:10.1021/acs.est.7b05045, 2018.

636   Zhu, W., Guo, S., Zhang, Z., Wang, H., Yu, Y., Chen, Z., Shen, R., Tan, R., Song, K., Liu, K., Tang,

637   R., Liu, Y., Lou, S., Li, Y., Zhang, W., Zhang, Z., Shuai, S., Xu, H., Li, S., Chen, Y., Hu, M.,

638   Canonaco, F. and Prévôt, A. S. H.: Mass spectral characterization of secondary organic aerosol

639   from urban cooking and vehicular sources, Atmos. Chem. Phys., 21(19), 15065–15079,

640   doi:10.5194/acp-21-15065-2021, 2021.

641   Zushi, Y., Hashimoto, S. and Tanabe, K.: Nontarget approach for environmental monitoring by GC ×

642   GC-HRTOFMS in the Tokyo Bay basin, Chemosphere, 156, 398–406,

643   doi:10.1016/j.chemosphere.2016.04.131, 2016.

644

645

646

647   **Graphic abstract**

648

649
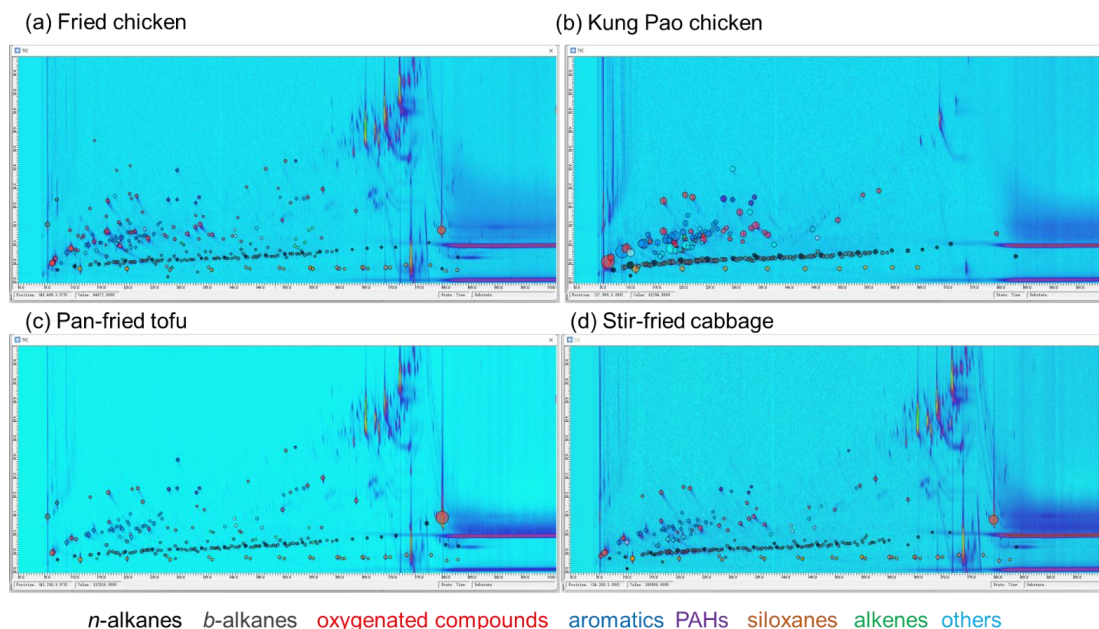
Atmospheric
Chemistry
and Physics

Discussions

650 **Figure Captions:**

651 **Figure 1.** Chemical identified from fried chicken (a), Kung Pao chicken (b), Pan-fried tofu (c), and

652 stir-fried cabbage (d) emissions. Column and Tenax TA bleeding after 75 min in 1st retention time are

653 excluded from qualification, quantification, and 2D binning processes. Blobs are colored by
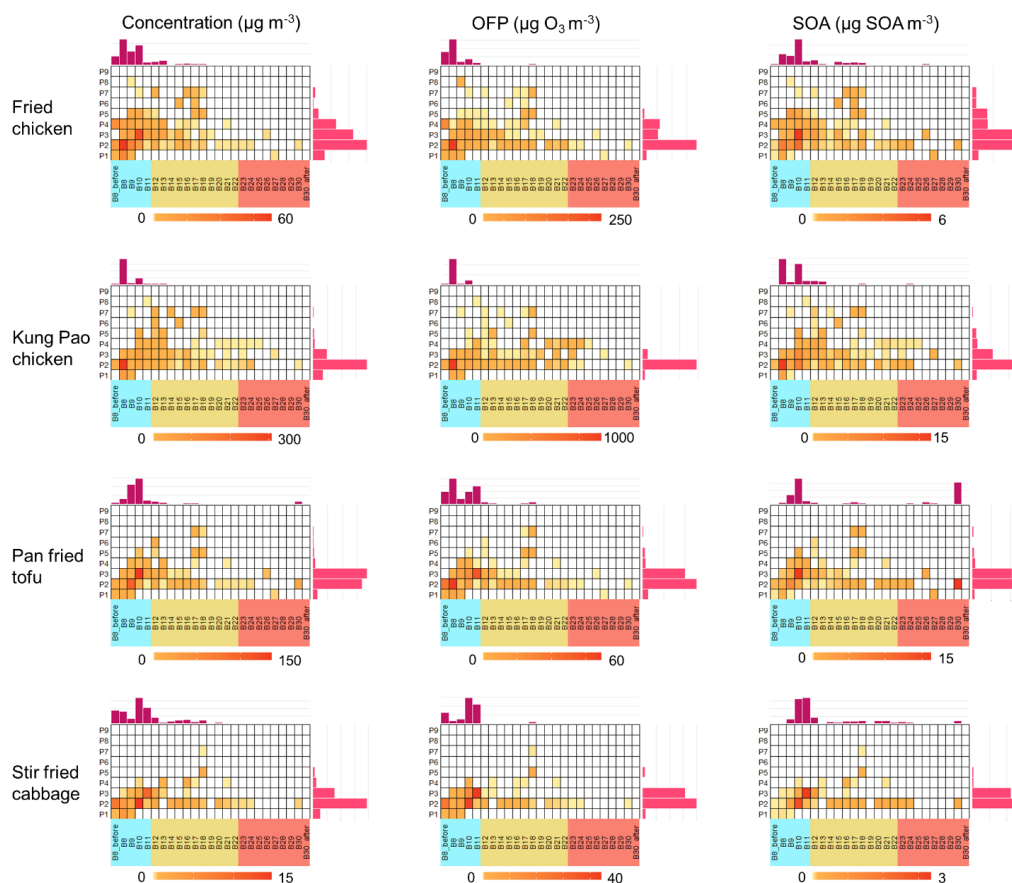
654 chemical groups.

655 **Figure 2.** Volatility-polarity panels of gaseous chemical emissions from fried chicken, Kung Pao

656 chicken, pan-fried tofu, and stir-fried cabbage fumes, and ozone formation potential (OFP), and

657 secondary organic aerosol (SOA) estimation from gas-phase precursors. VOCs (blue color in x-axis),

658 IVOCs (orange color in x-axis), and SVOCs (red color in x-axis) are displayed in volatility bins (a

659 decrease of volatility from B9 to B31) along with their polarity (an increase from P1 to P10 in y-axis).

660 The mass concentration unit is $\mu g \ m^{-3}$.

661 **Figure 3.** PLS-DA classification results of setting the cooking style (a) or oil (b) as grouping

662 variables. When oil was set as the grouping variable, the separation of groups was much better than

663 setting the dish as the grouping variable. The PLS-DA comparison result of cooking emissions and

664 oils is displayed in (c), indicating that the cooking fume is not just the evaporation of oil itself.

665 Positive loadings of oil and cooking fume chromatograms (d) demonstrated the key components

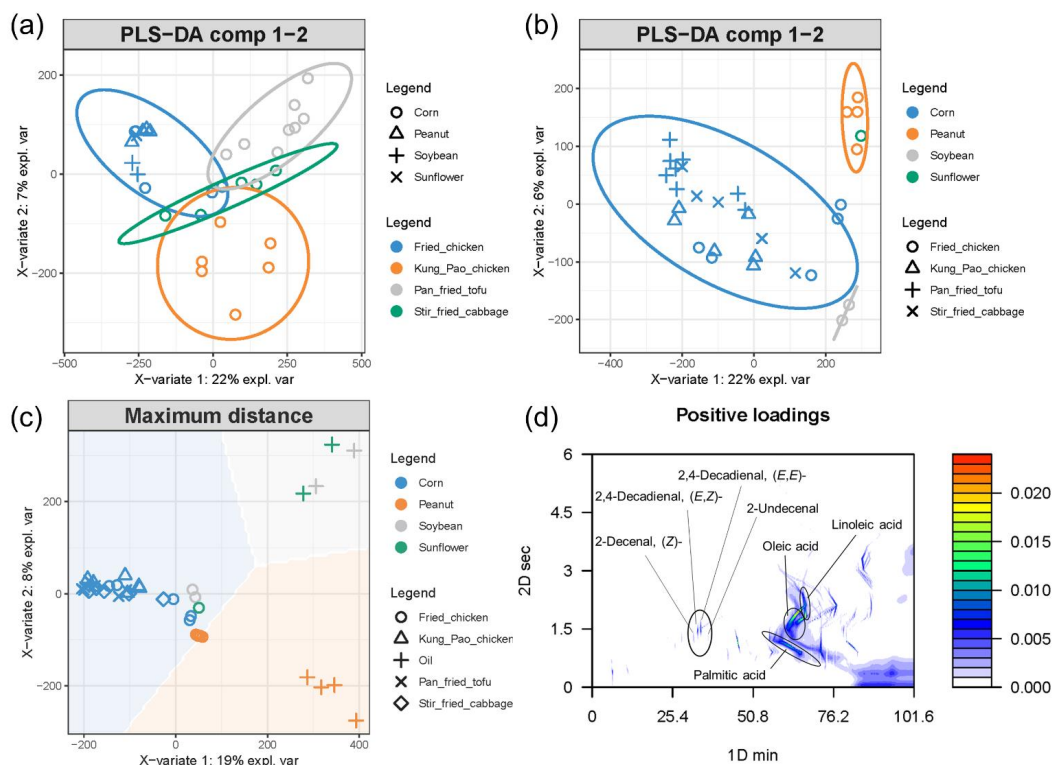666 contributing to the similarities of samples.

667

Figure 1. Chemical identified from fried chicken (a), Kung Pao chicken (b), Pan-fried tofu (c), and stir-fried cabbage (d) emissions. Column and Tenax TA bleeding after 75 min in 1st retention time are excluded from qualification, quantification, and 2D binning processes. Blobs are colored by chemical groups.

Figure 2. Volatility-polarity panels of gaseous chemical emissions from fried chicken, Kung Pao chicken, pan-fried tofu, and stir-fried cabbage fumes, and ozone formation potential (OFP), and secondary organic aerosol (SOA) estimation from gas-phase precursors. VOCs (blue color in *x*-axis), IVOCs (orange color in *x*-axis), and SVOCs (red color in *x*-axis) are displayed in volatility bins (a decrease of volatility from B9 to B31) along with their polarity (an increase from P1 to P10 in *y*-axis). The mass concentration unit is $\mu g\ m^{-3}$.

Atmospheric
Chemistry
and Physics
Discussions

Open Access

EGU

680

Figure 3. PLS-DA classification results of setting the cooking style (a) or oil (b) as grouping
variables. When oil was set as the grouping variable, the separation of groups was much better than
setting the dish as the grouping variable. The PLS-DA comparison result of cooking emissions and
oils is displayed in (c), indicating that the cooking fume is not just the evaporation of oil itself.
Positive loadings of oil and cooking fume chromatograms (d) demonstrated the key components
contributing to the similarities of samples.

687